thermoscientific

APPLICATION NOTE

4D STEM imaging using an Electron Microscope Pixel Array Detector (EMPAD)

Introduction

There is increasing interest in obtaining information from diffraction patterns taken at each point in spectroscopy mapping applications using a transmission electron microscope (TEM). These data not only provide new information and answers but are complementary and value additive to traditional spectroscopic mapping data such as Scanning Transmission Electron Microscopy (STEM) imaging & Energy Dispersive X-Ray analysis (EDX). In normal STEM imaging, only ring or disk areas of the diffraction pattern are recorded and the averaged intensity displayed in each point of the scan provides bright field and dark field imaging information. By acquisition of a diffraction pattern of each point of a scan (4D STEM), additional information becomes accessible for contrast optimization, e.g. strain or orientation mapping, E/B field measurements or even improvement of spatial resolution via Ptychography. For this approach, the limitations of conventional cameras need to be overcome like the low dynamic range, the low signal/noise ratio, the slow readout speed and the large amount of data to be handled. The principle of acquiring a 4D STEM map is illustrated in figure 1 (left). Depending on the digital aperture chosen, different information can be obtained as exemplified in a HAADF and center of mass image extracted from the diffraction patterns recorded at each image point. The increase in information is illustrated in Figure 2, which illustrates the difference between the information one can acquire with fixed geometrical STEM detectors compared to the pixelated detector.

The Thermo Scientific™ EMPAD detector is designed for diffractive STEM applications with its high dynamic range of 1 to 1 Million primary electrons per readout (Figure 3) , its high speed of 1100 fps and high DQE and MTF with 150 mμ pixel size in a matrix of 128x128 pixels. This application note shows the performance of the sensor in various use cases and illustrates the power of 4D STEM. For more information on the sensor please have a look at the product datasheet for the EMPAD detector.

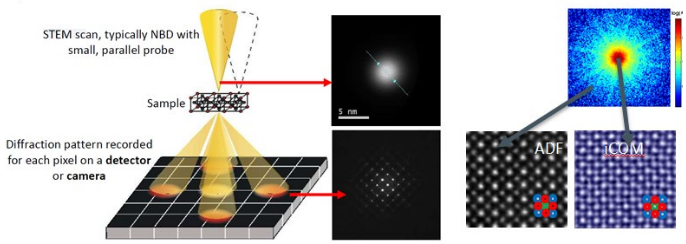

Figure 1. The Principle of a 4D STEM acquisition (left). In each point, the diffraction pattern is recorded and in post processing the image can be reconstructed as illustrated with HAADF and center of mass (COM) imaging of $SrTiO_3$ (right).

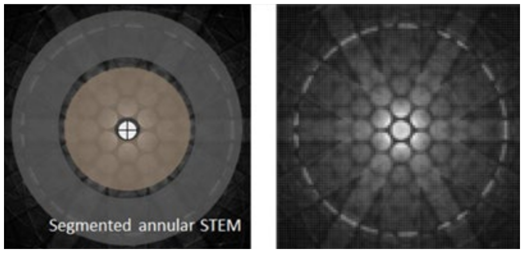

Figure 2. Comparison of which information is recorded using conventional STEM detectors (HAADF, BF and DF) and a pixelated detector in each image point of a scanned image.

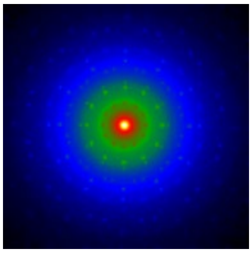

Figure 3. Diffraction pattern (log scale) of a double graphene layer @ 80kV. The central spot has 10^6 the intensity of the outer spots illustrating the huge dynamic range of the EMPAD detector.

ThermoFisher SCIENTIFIC

Simultaneous acquisition and post processing of complementary STEM images

When using a pixelated detector, the annular momentum transfer is conserved in each point of the scanned area and can be used to recover any STEM images using conventional (BF, DF, HAADF) or unconventional STEM imaging with masks not accessible with normal STEM detectors (typically disks or ring shapes). With post processing this allows interrogation of the data set to obtain perfectly synchronized complementary information on structure, fields, strain or orientation of the material.

An example of conventional STEM imaging is shown in Figure 4, where the information of ABF, BF, HAADF and iDPC is extracted from one data-set on $SrTiO_3$ in [110] projection exploiting the sensors high dynamic range for simultaneous bright and dark field imaging. Since the sensor has a linear response the intensities are easily quantifiable and can be used for obtaining quantitative information via simulations.

STEM imaging and phase mapping of precipitation in Alloy 718

Unconventional imaging using masks not provided by standard detector geometries can be used to identify new information. Figure 5 shows an example in STEM imaging. Here, different crystallographic phases of precipitates in alloy 718 can be identified. In the conventional imaging (BF, DF), the precipitates can be visualized, but the differences in crystallography cannot be resolved. Selecting the weak spots of the different phases next to the matrix reflections allows for the image to be colorized so that the three different species of precipitates can be identified. Even after the experiment, each image point in the diffraction pattern can be retrieved, so that further analysis is possible.

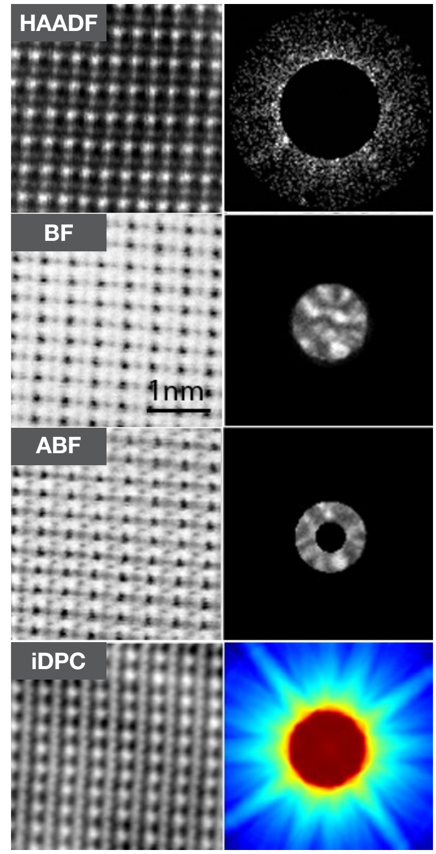

Figure 4. Reconstructed STEM images of $SrTiO_3$ in [110] projection using one data set acquired with a pixelated STEM detector. Post processing of the data allows for extracting various images with complementary information in one acquisition.

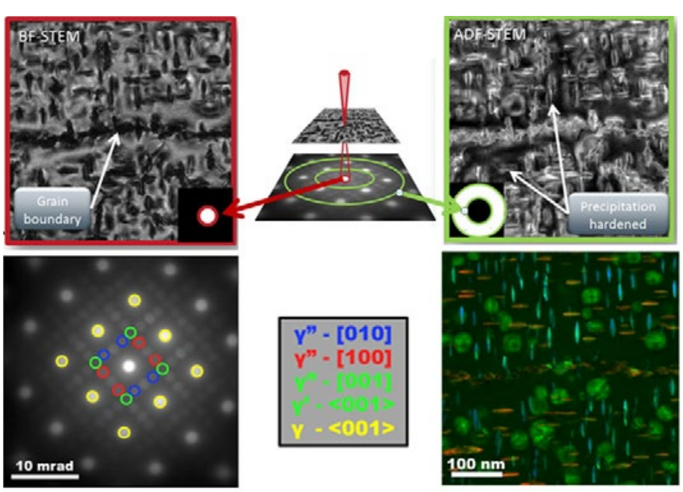

Figure 5. Experimental set-up to record a 4D STEM image of alloy 718 (upper left). The conventional BF and DF images can be extracted from the 4D data (upper part). By selecting three different classes of reflections (Red, Blue, Green) in the diffraction pattern (lower left), the location of the different precipitate classes can be identified in the image (lower right).
Sample Courtesy Prof. G. Burke, University of Manchester.

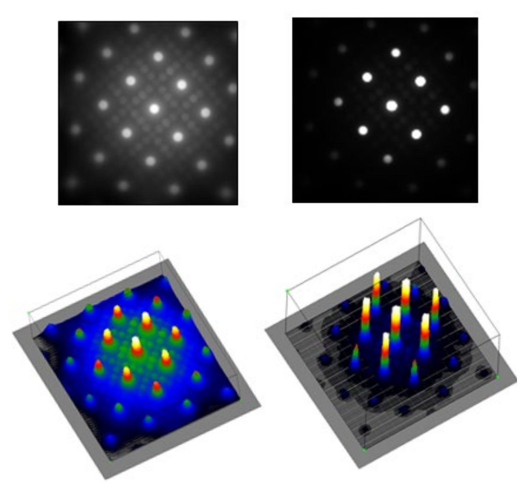

Figure 6. Logarithmic plot (left) and linear plot (right) of the summed intensities of 256x256 diffraction patterns of alloy 718. The high dynamic range required to record the metal matrix diffraction spots and the weak diffraction spots of the precipitates are illustrated.

Magnetic field visualization in LM STEM

The diffraction pattern not only gives access to structural information, but also field information on magnetic or electric fields can be obtained. Due to the Lorentz force acting on the electrons passing through in plane magnetic fields, the center of mass of the diffraction pattern is shifted. Figure 7 shows an example of a magnetic multilayer of 100 nm FeCoB / 4 nm AlN_{10}. The images are recorded in LM STEM mode to preserve the magnetic structure in the TEM. In the center of mass analysis the magnetization of the thin films are clearly detected, even stray fields in vacuum become visible in the false color representation.

The EMPAD is based on detector technology described in the publication 'High dynamic range pixel array detector for scanning transmission electron microscopy'; authored by Mark W. Tate, Prafull Purohit, Darol Chamberlain, Kayla X. Nguyen, Robert Hovden, Celesta S. Chang , Pratiti Deb , Emrah Turgut , John T. Heron, Darrell G. Schlom , Daniel C. Ralph, Gregory D. Fuchs, Katherine S. Shanks, Hugh T. Philipp, David A. Muller and Sol M. Gruner; in Microscopy and Microanalysis 22, 237-249.

DOI : http://dx.doi.org/10.1017/S1431927615015664

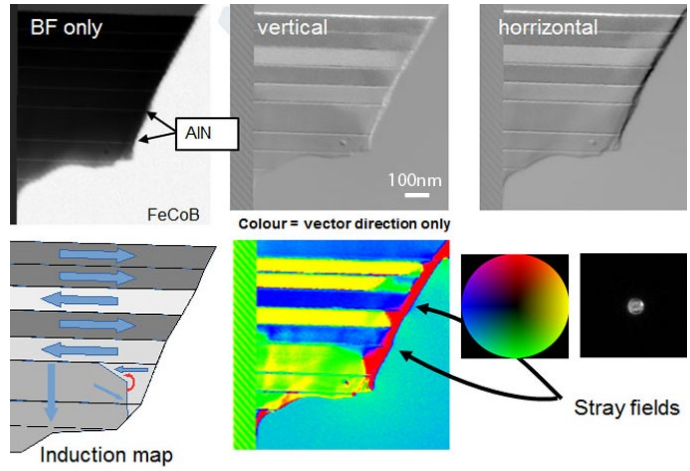

Figure 7. Bright field LM-STEM image of 100nm FeCoB / 4nm $(AlN)_{10}$ multilayer (upper left), vertical and horizontal shift of the center of Mass (upper left), false color representation of the magnetization of the different layer with model of the magnetization direction.
Sample courtesy: Prof. J. Zweck, University of Regensburg.

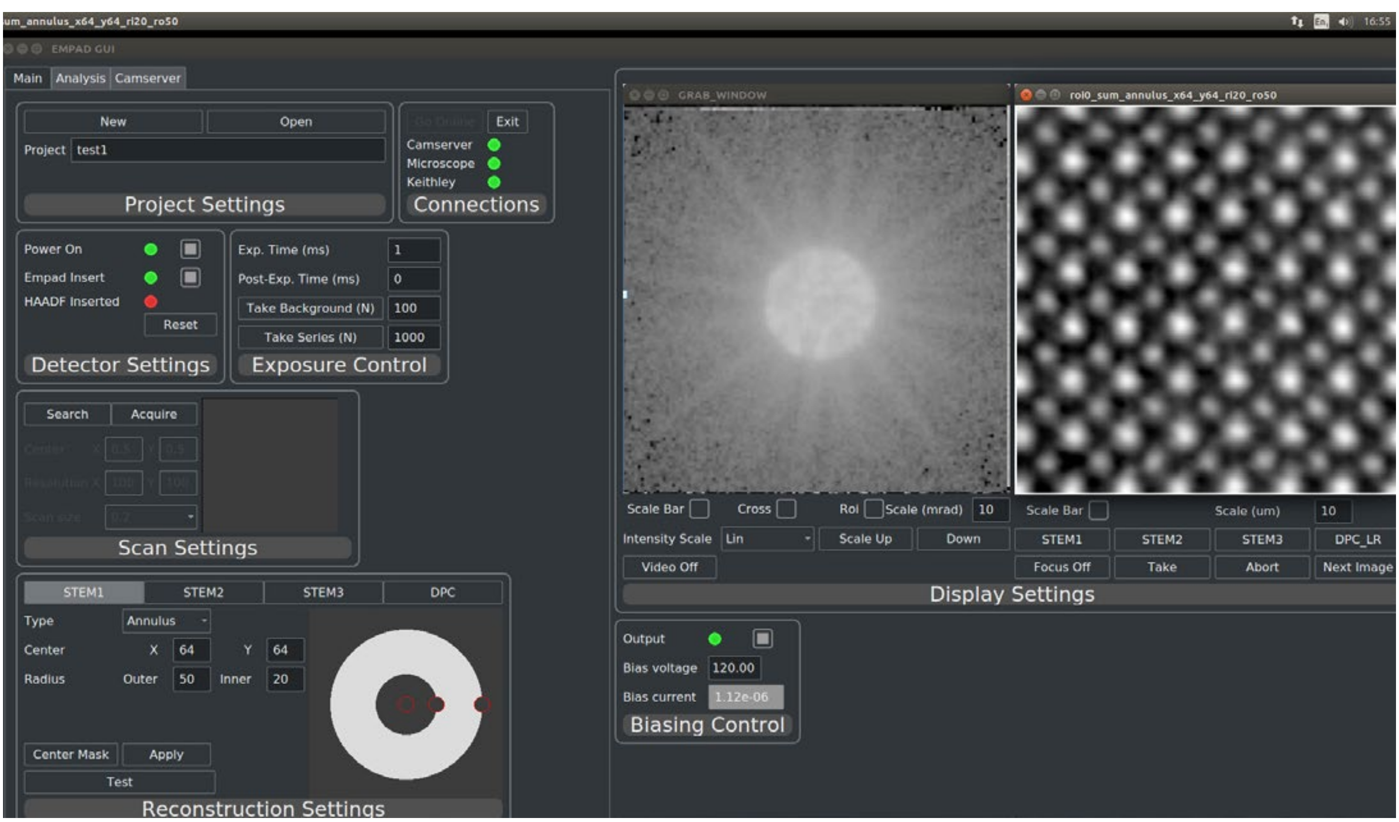

Figure 8. The graphical user interface of the EMPAD detector showing a diffraction pattern of $SrTiO_3$ (log scale) with reconstructed HAADF image using a user defined ring mask. The image is reconstructed 'live' during the acquisition.

thermo scientific

Notes

Find out more at **thermofisher.com/FEI**

Thermo Fisher SCIENTIFIC